Kufa Journal of Engineering
Vol. 17, No. 1, January 2026, P.P. 456-472
Article history: Received 30 November 2024, last revised 23 May 2025, accepted 23 May 2025

ENHANCING STABILITY THROUGH EXPERIMENTAL RESEARCH ON THE FLAPPED HORIZONTAL AXIAL WIND TURBINE

Qassim Wanis .M[1], Muhammad A.R.Yass[2], and Ahmed Kamil Hasan[3]

[1] Electromechanical Engineering Department, University of Technology, Baghdad, Iraq, Email:qasim.alkenany@gmail.com.

[2] Electromechanical Engineering Department, University of Technology, Baghdad, Iraq, Email:50251@uotechnology.edu.iq.

[3] Electromechanical Engineering Department, University of Technology, Baghdad, Iraq, Email:Ahmed.k.alali@uotechnology.edu.iq.

https://doi.org/10.30572/2018/KJE/170125

ABSTRACT

This study examines the effects of changing flap angles on the aerodynamic performance of a wind turbine blade, concentrating on torque coefficient (Cm), thrust coefficient (Ct), power coefficient (Cp), and power in watts over a range of rotational speeds. The results show that adding a flap considerably increases Cp and Cm, especially at low-to-moderate speeds. The maximum power and torque values are produced using a 6° flap. The 6° flap design in particular exhibits improved energy collection capabilities, with a maximum Cp gain of almost 20% above the baseline (0° flap). Notable gains in Cm are also seen, with the 6° flap offering a peak torque up to 25% greater than the baseline, indicating possible advantages for starter torque under specific conditions. at low wind speeds. A moderate flap angle of 4° increases thrust without overtaxing the blade structure at higher speeds, resulting in the best balanced improvement for Ct. The results show that a flap angle of 4° offers the best balance, boosting stability and efficiency; however, larger angles (6°) may cause excessive drag and structural loads at high speeds. German cod is used to calculate the geometrical data.According to this study, wind turbine blade design is optimized for better performance in low wind speed conditions.

KEYWORDS

Horizontal Wind Turbine (HAWT), Multi Section Wind Turbine Blade, design winglet, design fences, flaps.

1. INTRODUCTION

Wind energy has emerged as a pivotal renewable energy source, contributing significantly to the global pursuit of sustainable power generation. Axial wind turbines play a crucial role in harnessing wind energy efficiently, with their performance directly impacting the viability and effectiveness of wind energy systems. However, challenges such as stability and efficiency persist in the operation of axial wind turbines, particularly concerning the aerodynamic behavior of their blades. This study delves into the innovative application of flaps, winglets, and fences to enhance the stability and efficiency of axial wind turbines equipped with multi-section blades. Flaps strategically positioned along the blade span, offer opportunities for optimizing aerodynamic performance by modifying airflow characteristics. Similarly, In order to reduce flow disruptions and enhance overall turbine stability, winglets and fences are incorporated, thereby enhancing power generation efficiency. The exploration of these advanced technologies presents an exciting avenue for advancing the capabilities of axial wind turbines By leveraging the synergistic effects of flaps, winglets, and fences, A number of creative techniques have been employed by some of this field's researchers to successfully increase turbine efficiency, including. (Lei Xi, 2022) used a set of airfoils from the NACA series and organized and distributed them based on the thickness and curvature of each airfoil and created a new blade that differed from the individual blades taken in the experiment. The german cod was used to evaluate and analyze the blades' aerodynamic performance. The final results reveal that the use of complex multi-airfoil modeling may increase The wind energy utilization factor of the wind turbine blade is from 0.46 to 0.49. (Amer H.Muheise, 2021) investigated a comparative analysis of the behaviors and comprehensive performance of various blades, employing the NACA4412 single-cross-section HAWT blade with identical dimensions as a benchmark. Furthermore, it examines the performance and behavior of a multi-cross-section blade configuration both with and without the integration of fences. Utilizing multi-cross-section HAWT blades instead of single-cross-section blades results in an 8% augmentation in power coefficient (equivalent to 40 W) for a small wind turbine boasting a diameter of 127 cm and an output power of 500W.The experimental placement of gates on multi-section blades was meticulously determined, yielding a remarkable 16% enhancement in the overall power coefficient coupled with outstanding flutter stability, thus demonstrating the efficacy of the incorporated fences. (Vahid Akbari, 2022) divided the turbine blade into two parts, where the first section is in which the ratio is $r/R<0.52$, or in which the majority of the turbine's energy is concentrated, as he increased the chord length and twist angle in it and the second section is in which the ratio is $r/R > 0.52$, is the section concentrated. In which the

generation of starting torque kept it in its ideal condition, the results showed a decrease in the power factor by 1.5%, with this accompanying the rotation of the wind turbine at a speed of 4 m/s instead of 6 m/s. (Zhang et al, 2024) established a tidal turbine model utilizing (CFD), a methodology validated through experimentation in a flume. Subsequently, this study examines the dynamic effects on turbine blade performance, incorporating varying winglet lengths and cant angles. The investigation reveals that optimal blade performance is attained with a winglet cant angle of 45°, yielding approximately an 11% enhancement in efficiency and an approximate 8% increase in axial force. Furthermore, a positive correlation is observed between winglet length and performance improvement. Additionally, the research elucidates that the efficacy of a winglet in reducing blade load fluctuations stems from its displacement of the tip vortex generation position away from the blade rotation plane, rather than a reduction in tip vortex intensity. (Abdelghany et al, 2023) studied the effect of adding winglet at tip airfoil to a NACA4418 turbine blade. The blade radius is 0.36 m, the winglet dimensions fixed cant angle = 90^0, and length is variable as follows (0.008, 0.02, 0.04, 0.05, 0.06, 0.07) m, and the design tip speed ratio is fixed. It is 4.92.Overall, the results showed that the use of the winglet increased the performance of the turbine rotor. lift-to-drag ratio (*CL/CD*) and power coefficient. (Osama A.Gaheen, 2021) The research looked at the effects of winglet height (4–12)cm, cant angle (30^0–70^0), twist angle (1^0–5^0), and taper ratio (0.2-1) on wind turbine performance. Turbine power was more affected by H and θ than by β and Λ. Power output of a wind turbine is increased by 2% to 30% when winglets are added. According to the design, the maximum power increase is H = 8%R, $\theta = 30°$, $\beta = 3°$, and $\Lambda = 0.8$.

The purpose of this study is to discuss long-term problems with turbine efficiency and stability. The development of more reliable and effective wind energy systems will be made possible by experimental research and analysis, which will offer crucial insights into the effectiveness of these improvements. By using flaps and winglets on a multi-section turbine blade to increase the sustainability and efficiency of axial wind turbines at low wind speeds, this research seeks to expedite the development of wind turbine technology.

2. METHODS USED

A thorough technique is required to evaluate the effects of these design changes on the turbine's performance in the experimental investigation of flapped horizontal axial wind turbines for improved stability by utilizing a fence and winglet. The design and construction of the experimental setup, the measurement and analysis of aerodynamic forces, and the assessment of stability and performance indicators are all important components of the process.

A scaled-down version of a horizontal axial wind turbine with a winglet and fence makes up the experimental setup, which is exposed to regulated wind flow in a wind tunnel. To guarantee the precision and dependability of the experimental findings, the scaled model's design and construction are essential. To provide a representative and useful experimental setup, the turbine, fence, and flap's size and specifications are carefully chosen based on computer models and initial testing. To determine the effect of the fence and winglet on the flow field and turbine performance, aerodynamic force measurements are made. When employing the fence and winglet, a variety of sensors and equipment are used to record the wind speed and the number of turbine blade revolutions, such as an anemometer to record wind speed and a tachometer to monitor turbine blade rotations.These measurements allow the determination of the forces applied by the wind flow and offer useful information on the aerodynamic behavior of the redesigned turbine layout. To determine how well the fence and winglet improve the horizontal axial wind turbine's stability, stability and performance parameters are analyzed. The performance of the modified turbine is compared with that of a traditional HAWT by analyzing parameters such power output, thrust coefficient, tip speed ratio, and turbulence response.

3. MODEL OF MATHEMATICS

The fluid's velocity rises from zero at the boundary surface to a terminal value across a thin boundary layer. The boundary layer refers to the thin layer of fluid at the boundary surface when the fluid's velocity increases from zero to a terminal value. The design boundary layer Fig.1. equations are as follows (Elbashbeshy et al., 2022; Stabilisation of Hydrodynamic Instabilities, 2023; Jha & Samaila, 2023).

$$\text{Drag force, } F_D = \frac{37}{315}\rho b U^2 \delta \quad (1)$$

$$\text{Displacement thickness, } \delta = 5.835\frac{X}{\sqrt{Re}} \quad (2)$$

$$\text{Reynolds number(Re)} = \frac{UL}{v} = \frac{\rho UL}{\mu} \quad (3)$$

$$\text{Shear force, } \tau = 0.343\frac{\mu U_\infty}{X}\sqrt{Re} \quad (4)$$

$$\text{Drag coefficient, } C_D = \frac{1.371}{\sqrt{Re}} \quad (5)$$

The power coefficient (Cp)of a wind turbine is defined and is related to the Betz Limit.

$$Cp = \frac{P}{\frac{1}{2}\rho V^3 A} = \frac{\text{power of Rotor}}{\text{power of Wind}} \quad (6)$$

$$Cp = 4a(1-a)^2 \quad (7)$$

The maximum Cp is then calculated from the power coefficient derivative with respect to a equated to $\frac{V_2}{V_1} = 1/3$ (8)

$$Cp_{max} = \frac{16}{27} = 0.5926$$

where wind speed upstream of the turbine $is\ V_1$ and the downstream is V_2 (Volpiani, 2021 ; Umar et al, 2022).

4. FLAPS

Flaps are a high lift mechanism made up of moveable panels that are fastened to the blade's trailing edge. In most cases, their expansion increases the camber, chord, and surface area of the wing. As a result, lift and drag rise and the stall speed decreases (Calì et al, 2022).

4.1. The main function of the flaps

The Principle work of flaps for wind turbines is to control the aerodynamic performance of the blades by changing their shape and camber. Typically fastened to the trailing edge of the blades, flaps can be extended or retracted based on the desired power production and wind speed. By modifying the lift and drag forces, flaps may also be employed to lessen the strains on the tower and blades. (Jung & Schindler, 2020). Particularly in areas with low wind speeds or complicated topography, flaps can significantly affect the efficiency and dependability of wind turbines. By improving the lift-to-drag ratio and postponing the stall onset, flaps can raise the power coefficient and yearly energy production of wind turbines. By reducing the gust response and lessening the impacts of wind shear and turbulence, flaps can help lessen the fatigue and high pressures on the tower and blades. Flaps are one type of flow-control device that works to enhance wind turbine aerodynamics by adjusting the wake and boundary layer. (Afify et al, 2024; Bing, 2017).

5. FENCE

Fences are built as parallel plates to the blade root to prevent span-wise flow generation to new tips (Gopinathan & Rose, 2021). the boundary layer on the blade radius often drifts in the first and third quarters of the blade radius due to span-wise flow. A side force that the span-wise flow exerts on the fences produces a trialing edge vortex. By combining fresh air, this vortex attempts to lessen the thickness of the boundary layer and inhibit span-wise flow, which lowers induce drag and raises the lift coefficient of the over panel (Das & Samad, 2020).

6. WINGLET

Winglets are aerodynamic devices attached to the tips of wind turbine blades as shown in Fig.4, designed to improve their performance. By reducing the vortices generated at the blade tips, winglets minimize the loss of efficiency caused by aerodynamic drag, thereby increasing the turbine's power output. They work by redirecting airflow to reduce swirling motion, which in turn decreases induced drag and improves the overall efficiency of the turbine Winglets in wind turbine design have been the subject of extensive research and development due to their potential to significantly improve turbine efficiency and performance. By mitigating the adverse effects of blade tip vortices, winglets reduce aerodynamic losses and enhance power generation, particularly at low wind speeds. Furthermore, the integration of winglets can

contribute to the overall stability and reliability of wind turbines by reducing fatigue loads on the blades and extending their operational lifespan (Nair et al., 2020; Mohamed et al., 2021; Ala, 2024).

7. EXPERIMENTAL CONFIGURATION

The best and most ideal settings for combining the maximum power generated and the peak power absorbed by the blade from the free stream were determined by calculating all aerodynamic and technical concepts. Table 1 demonstrates the high operational power coefficient of wind turbine blades. The specifications of the small wind turbine model with three multi-cross-section blades are provided by the specification of the used HAWT. Table 2 displays the blade geometry of the multi-airfoil cross-section; each segment is specified by its location, chord, twist, and airfoil. The design used SolidWork Package Design Tools for 3D Building Wind turbine blade geometry. The best tool for 3D construction is a 3D printer. PLA was used to manufacture wind turbine blades, which could weigh up to 205 g apiece. As seen in Figs. 1 and 2, a multi-cross-section blade is split into three portions before being gathered together. In order to regulate the angle of the flaps, as seen in Fig.3, the flaps are connected to a digital servo and connected to a potentiometer using an STM32 microcontroller. After that, fences were positioned in accordance with the developed model. As shown in Table 3, dimensions and measurements are established. The fences were positioned at the end of the first third and the beginning of Each blade features many cross-sections in the latter third. This is This is carried out due to the first third's large flow area, which causes. the path to divert in the direction of the initial extended flow. The last third is to stay away from peripheral vortices that cause heave and flutter. It causes drag. The fence heights were calculated using conjecture. The blade's radius is threaded with black. Establish flow corridors and fencing at the primary locations. The intricate winglet design is attached to the tips of each feather on wind turbine blades, as seen in Figs. 4, 5, and 6. Fig.7 displays the dimensions of the winglet, and Fig.8 depicts the winglet in a 3D printer. Fig.9 illustrates the design of multi-section blades with winglets using Solid Works programs. In every investigation, As shown in Fig.10, the fences and wings were fastened to the multi-section turbine blade using flaps. The performance of the wind turbine's wings and fences is compared in each experiment; the first uses fences, while the second uses flaps in a wind tunnel. Additionally, as seen in Fig.11, an anemometer was used to track wind speed. The number of turbine spins was measured using tachometer devices, as seen in Fig.12.

7.1. Educational Wind Tunnel (EWT) Operations Manual

As seen in Fig.13 The AEROLAB Educational Wind Tunnel is of the Eiffel, or Open Circuit,

type with a 12x12x24 -inch (30.48cm x 30.48cm x 60.96cm) test section. Clean-tunnel (empty test section) top speed is in excess of 145 mph (64.8 m/s) The 9-blade fan is constructed of fiberglass-reinforced plastic designed for a maximum rotational speed of 3437 rpm (rotations per minute). As used in the EWT, the fan operates at a maximum speed of 2345 rpm. It is mounted directly to the shaft of a 10HP (7.46 kW) motor. The motor speed is controlled by a heavy-duty variable frequency drive, or VFD. The VFD is described in the manufacturer's manual and was commissioned at AEROLAB by an authorized factory technician.

Table 1. Specification of used HAWT

Rotor		Blade	
Rotor Diameter	1.251 m	Blade Span	0.56 m
Hup Diameter	0.13 m	Base Chord	0.113 m

Table 2. Blade geometry of multi airfoil cross- section

POS(mm)	Chord Length mm	Twist Angle (Degree)	Foil
0	113.46	30.92	FX 66 -S-196 V1
18.680	109.63	24.88	FX 66 -S-196 V1
68.680	95.83	19.86	FX 63 -137 S
118.680	83.81	14.36	FX 63 -137 S
168.680	73.77	11.96	SG6043
218.680	64.59	9.65	SG6043
268.680	57.09	7.99	SG6043
318.680	50.77	6.75	SG6043
368.680	45.14	5.77	SG6043
418.680	40.77	4.99	SG6043
468.680	37.03	4.36	SG6043
518.680	35.44	3.82	SG6043
549.060	34.49	3.54	SG6043
552.100	34.08	3.52	SG6043
554.41	32.2	3.5	SG6043
557.44	27.7	3.47	SG6043
558.89	24.18	3.46	SG6043
560.05	20.03	3.45	SG6043
560.92	12.33	3.44	SG6043

Fig.1. Multi Cross-Section Three Blade With Flaps Printed in 3D Printer (back

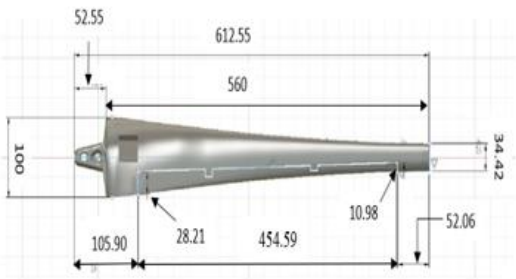

Fig.2. Dimension Multi Cross-Section Blade With Flaps (Al Dimension in mm)

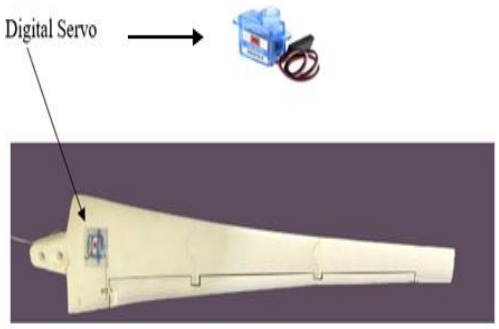

Fig. 3. Multi section blade with flaps connected with digital servo.

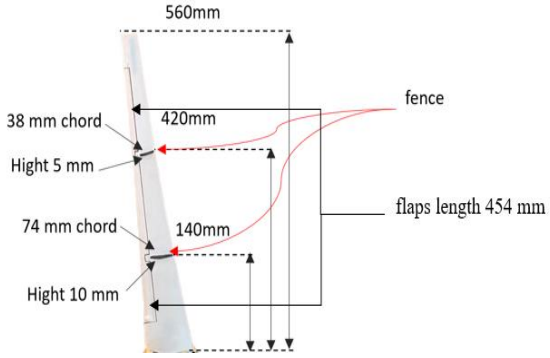

Fig.4. Dimensions of the fence installation places(front of side).

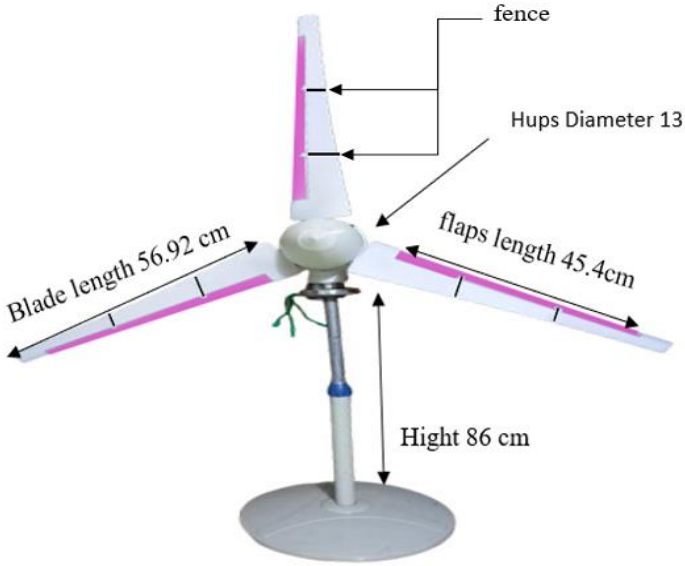

Fig. 5. Full scale Flapped Horizontal Axial Wind Turbine blade with fences

Fig. 6. To scale flapped horizontal axial wind turbine blade rotor diameter 25 cm with fences in aerolap education wind tunnel system .

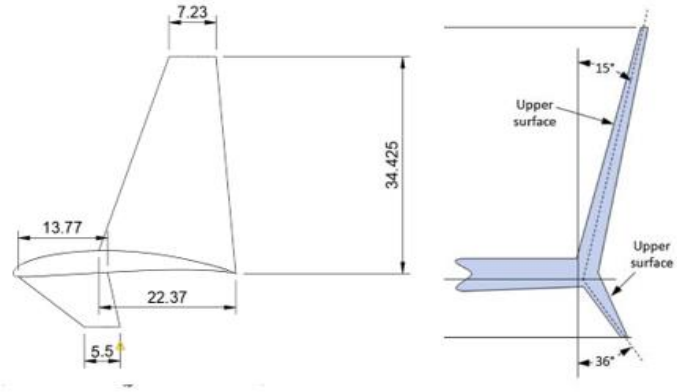

Fig. 7. Dimension winglet (mm)

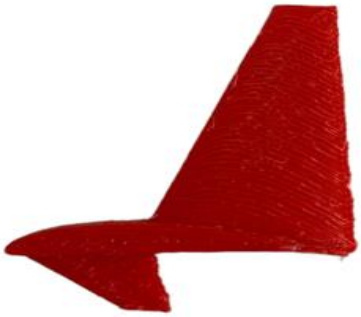

Fig.ure 8. 3Dprinter winglet

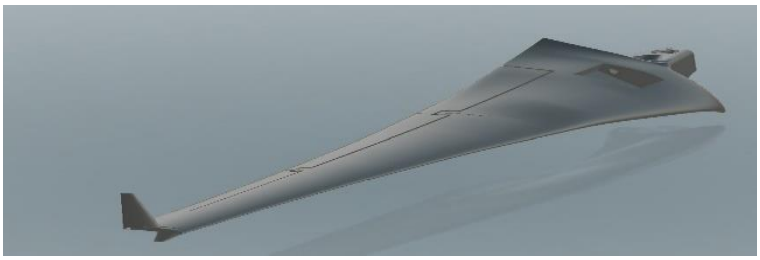

Fig.9. SolidWorks Flapped multi section blades with winglet

Fig.10. to scale Flapped Horizontal Axial Wind Turbine blade rotor diameter 25 cm with winglet

Fig. 11. Anemometer Digital

Fig.12. Digital Laser Tachometer

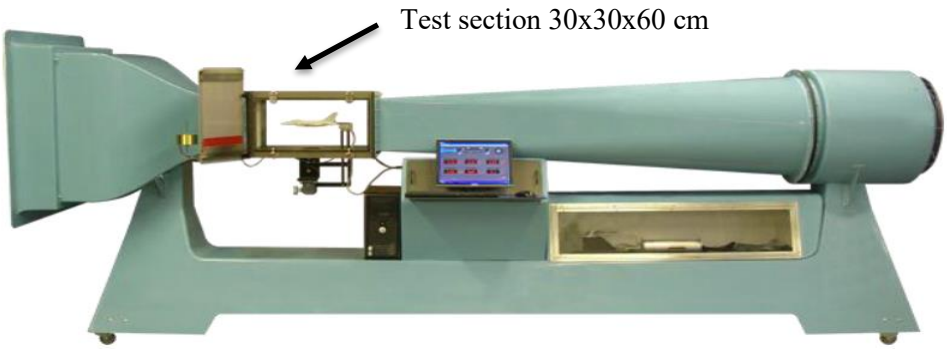

Fig. 13. Educational Wind Tunnel (EWT) Operations Manual

8. RESULT AND DISCUSSION

This Fig.14 shows the relationship between the Torque Coefficient (Cm) and the Rotational Wind Speed (rpm) for a wind turbine under different flap conditions. the curves represent different flap angles and the corresponding performance of the turbine The torque coefficient (Cm) is a measure of how effectively the wind turbine generates torque (rotational force) from the wind. It is crucial because torque is what drives the turbine's rotor to turn and generate electricity. A higher (Cm)value indicates better torque generation. In this graph, (Cm)values range from approximately 0.04 to 0.16. As the rpm increases, the torque generation capability of the turbine changes, which is reflected in the (Cm)values. Each curve represents the torque performance of the turbine at different flap angles: Without Flap curve represents the baseline performance of the turbine without any flap. The torque coefficient starts around (Cm approx. 0.04) at low rpm and reaches a peak of approximately (Cm = 0.11) at around 100 rpm. After this point, the (Cm)decreases as the rpm increases. Flap Angle 2° curve represents the turbine performance with a 2° flap angle. At low rpm, the torque is similar to the turbine without a flap. However, at mid-range rpm (around 80-120), the torque performance is slightly better than the no-flap configuration, peaking just above (Cm = 0.12), before it declines. Flap Angle 4° line shows the turbine's performance with a 4° flap angle. With a peak (Cm) of around 0.148, it produces significantly more torque at mid-range rpm (roughly 70–150), outperforming both the 2° and no-flap scenarios. The turbine with a 6° flap angle is shown by the Flap Angle 6° line. With a peak torque of about (Cm = 0.16), this design is the most effective flap angle in terms of torque production. Nevertheless, the graph indicates that as the rpm rises over 150, torque falls after hitting this high. The most torque is produced by a turbine with a 6° flap, which is followed by one with a 4° flap, one with a 2° flap, and one without a flap. Every arrangement has a torque peak between 100 and 150 rpm, after which it starts to decrease, showing a boundary in the torque generation's effective range. At some operating speeds, the installation of a flap greatly enhances torque output in the turbine, particularly at higher angles. However,

as the fall following the peak illustrates, too high flap angles or rpm can lead to diminishing results. All variants exhibit a decrease in torque as rpm increases after reaching a peak (Cm). This implies that regardless of the flap angle, the aerodynamic forces acting on the blades are less effective in producing torque at high rotational speeds. This graphic illustrates how torque output is enhanced by wind turbine blade flaps, with the 6° flap being the most efficient. There is a trade-off, too, as performance declines with increasing rpm. Comprehending this relationship is key for optimizing turbine operation, particularly at varying wind speeds and rotor speeds. In the current research, based on the design of the turbine blades and the wind turbine under test conditions, The Thrust Coefficient (Ct) for a wind turbine under various flap configurations is shown against Rotation Wind Speed (rpm) in Fig.15. The axial force (thrust) that the wind exerts on the wind turbine rotor is measured by the thrust coefficient (Ct). It is essential for assessing the structural stresses on the turbine and can reveal how well the turbine harnesses wind energy. The thrust coefficient of the turbine at various flap angles is shown by each curve. The thrust coefficient begins at (Ct = 0.2) in the absence of a flap line and gradually increases. The curve shows that as the rpm increases, the thrust also increases, reaching approximately (Ct = 0.9) at high rpm. This configuration provides the baseline against which the other flap configurations can be compared. at flap angle of 2°. Compared to the no-flap configuration, the thrust generation is similar at low rpm but starts to perform slightly better at higher rotational speeds, reaching a (Ct) just above 1. at Flap Angle 4°This configuration shows improved thrust performance across most of the rpm range, starting similarly to the other cases at low rpm but providing noticeably better thrust as rpm increases. It reaches a maximum (Ct) value of around 1.15 at higher rpm.This suggests that the 4° flap angle improves the turbine's ability to capture wind energy and generate thrust. at Flap Angle 6°. At low to mid rpm, this configuration performs similarly to the 4° flap. However, at higher rotational speeds (around 150 rpm and above), the thrust coefficient improves significantly, reaching the highest (Ct) values of the configurations (around 1.1). This indicates that the 6° flap angle is the most effective at increasing thrust at high rotational speeds, although it may also lead to higher structural loads. The Fig.16 shows the relationship between the power coefficient (Cp) and the rotational wind speed (measured in rpm) for a wind turbine under different conditions. The curves in the figure represent various configurations of a turbine blade with and without flaps at different flap angles.

The figure demonstrates that introducing flaps and varying their angles significantly affects the aerodynamic performance of the wind turbine. Increasing the flap angle improves the power coefficient up to a certain point, after which the benefits diminish, particularly at higher rpm.

The Fig.17 represents the relationship between the power output (in watts) of a wind turbine blade and its rotational wind speed (in RPM) under different flap angle configurations. The graph compares the performance of the turbine blade with no flap (represented by the red line) to configurations with flap angles of 2°, 4°, and 6° , respectively. Higher flap angles result in better power performance, with the 6° flap yielding the best overall results in terms of power output.

The power increases non-linearly with RPM . All configurations show a rapid increase in power from 50 RPM to around 150 RPM, after which the curves start to level off. Flaps enhance the aerodynamic performance of the blade by redirecting airflow more efficiently, resulting in higher power output compared to the no-flap scenario. This graph suggests that adding flaps, especially with higher angles (like 6°), can significantly improve the efficiency of the wind turbine blade by enhancing the power output at various rotational speeds.

Featuring a tip speed ratio of 6, wind speed (in wind tunnel test) of 2 m/s and angle of attack of 6^0, the empirical findings suggest that fences surpass winglets in terms of improving efficiency and stability, as illustrated in Table. They improved turbine performance at wind speeds between 5 and 13 m/s in contrast to studies by (RahnamayBahambary et al., 2024; Gall et al., 2022; Alyousuf & Korkmaz, 2023). Our results indicate that the current study employed a unique strategy to improve performance at 2 m/s, which is represented by the usage of fence and winglet-equipped flaps.

Table 3 Experimental Results from wind tunnel test.

Flapped Blade With Fence

Flap Angle (degree)	Wind speed (m/s)	Rotation speed (rpm)	Lift coefficient (CL)	Drag coefficient (CD)	Ratio CL/CD	Power coefficient (Cp)
2	2	193	2.54	0.0156	162	0.516
4		204	2.72	0.0147	184	0.529
6		218	3.04	0.0313	97	0.549

Flapped Blade With Winglet

Flap Angle (degree)	Wind speed (m/s)	Rotation speed (rpm)	Lift coefficient (CL)	Drag coefficient (CD)	Ratio CL/CD	Power coefficient (Cp)
2	2	188	2.42	0.0166	145	0.512
4		199	2.55	0.0151	168	0.522
6		210	2.89	0.0314	92	0.538

Plain Blade (Without Fence And Winglet)

Wind Speed (M/S)	Rotation speed (rpm)	Lift coefficient (cl)	Drag coefficient (cd)	Ratio Cl/cd	Power coefficient (cp)
2	183	2.34	0.0167	140	0.501

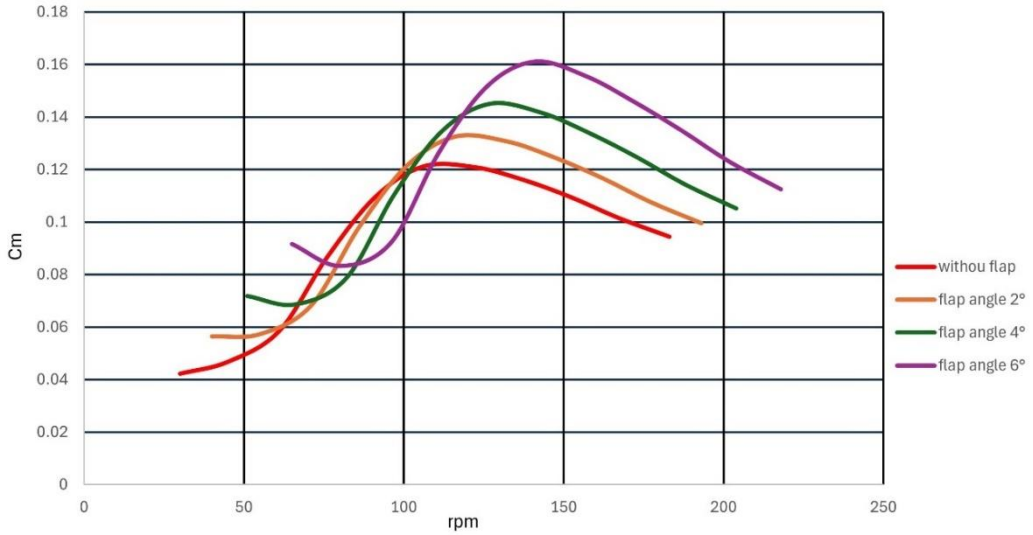

figure (14) Torque Coefficient (Cm) verses Rotation Wind Speed(rpm)

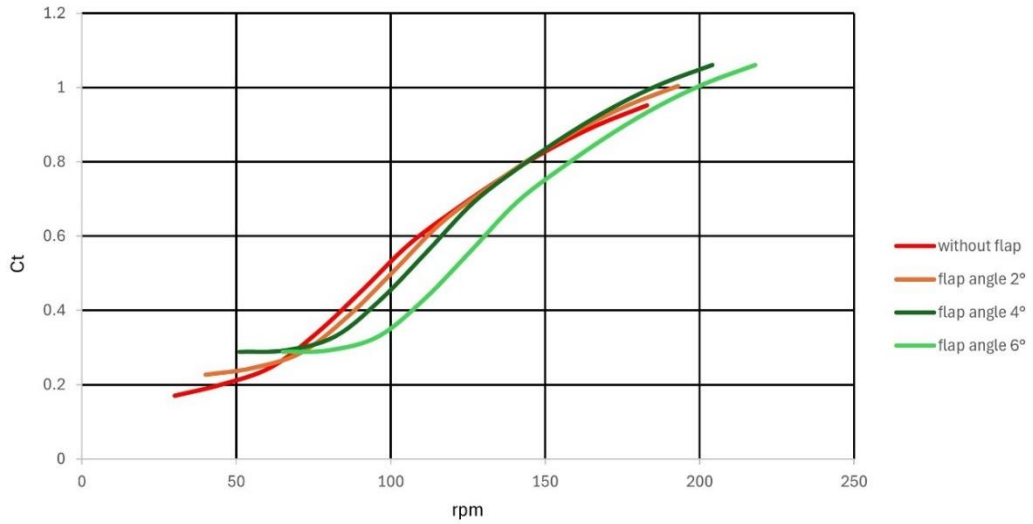

figure (15)Throust Coefficient (Ct) verses Rotation Wind Speed(rpm)

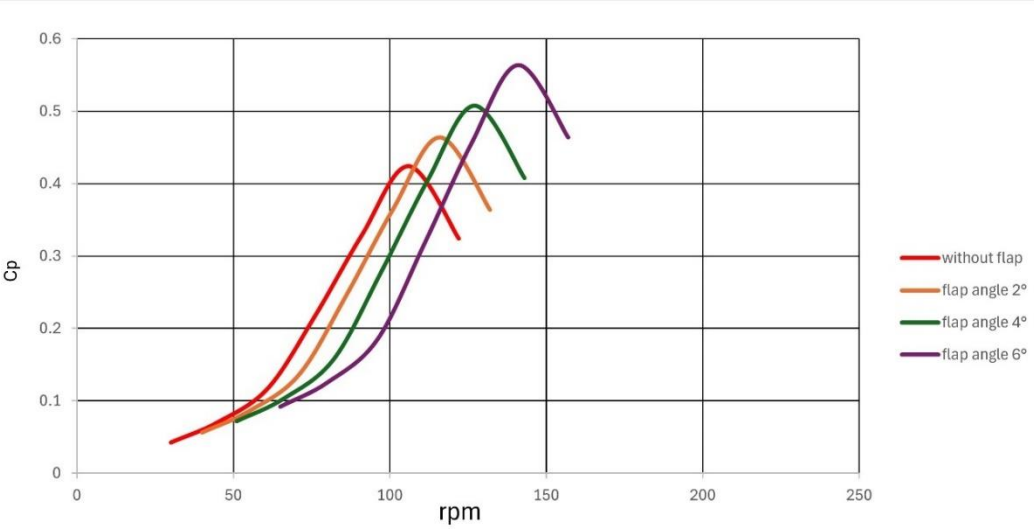

figure (16) Power Coefficient (Cp) verses Rotation Wind Speed(rpm)

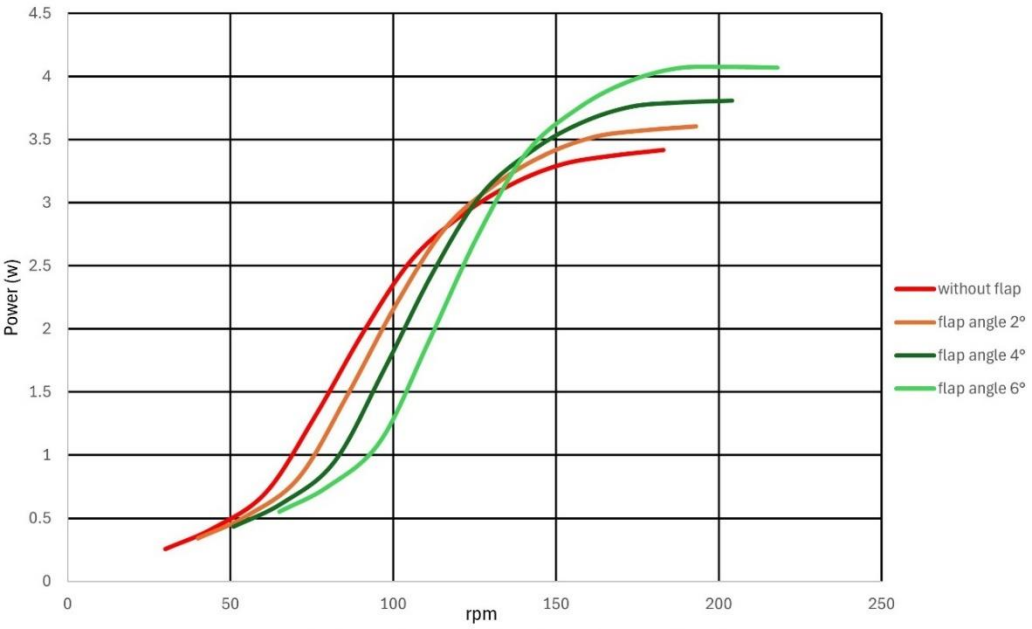

figure (17) Power (w) verses Rotation Wind Speed(rpm)

9. CONCLUSION

The Figs. 14,15,16 and 17 illustrate how varying flap angles impact torque coefficient (Cm), thrust coefficient (Ct), power coefficient (Cp) and Power in watt of a wind turbine blade across different rotational speeds (rpm). As flap angle increases, Cp and Cm show significant improvements, with the highest efficiency and torque achieved at a 6° flap angle, especially in the low-to-moderate rpm range, enhancing energy capture and torque generation. However, higher flap angles, particularly at 6°, lead to diminishing returns at elevated rpm due to increased aerodynamic drag and potential flow separation. In terms of Ct, the 6° flap adds more drag, which affects thrust consistency at high speeds, but the intermediate flap angles of 2° and 4° offer a steady rise in push without overtaxing the blade structure. Overall, a 4° flap angle appears to strike an optimal balance, It is especially appropriate for low-wind-speed circumstances and aligns well with the objective of improving both efficiency and stability in such settings by increasing torque and efficiency while preserving structural stability and reducing drag.

ACKNOWLEDGEMENT

I spoke with several researchers, academics, and practitioners while writing this study. They have contributed towards my understanding and thoughts. In particular, I wish to express my sincere appreciation to my main paper supervisor, Professor Dr. Muhammad A.R Yass, for encouragement, guidance, critics and friendship. I am also very thankful to my co-supervisor Professor Dr Ahmed Kamil Hasan for their guidance, advices and motivation. Without their continued support and interest, this Paper would not have been the same as presented here.

Funding Statement

The authors received no specific funding for this study.

Author Contributions

Muhammad A.R.Yass conceived the study.And Qassim Wanis .M.developed the theoretical framework and performed the experiments. Ahmed Kamil Hasan. aided in the analysis and supervised the project. All authors discussed the results and contributed to the final manuscript.

Availability of Data and Materials

The data that support the findings of this paper are available from the corresponding author upon reasonable request.

Conflicts of Interest

The authors declare that they have no conflicts of interest to report regarding the present study.

10. REFERENCE

Abdelghany, E.S., Sarhan, H.H., Alahmadi, R. and Farghaly, M.B. (2023) 'Study the effect of winglet height length on the aerodynamic performance of horizontal axis wind turbines using computational investigation', Energies, 16(13), p. 5138.

Afify, R.S., Idris, I.I., Eldrainy, Y.A. and Zidane, I.F. (2024) 'Enhancing efficiency of H-Darrieus wind turbines through experimental and numerical investigations of double darrieus configurations', Journal of Advanced Research in Applied Sciences and Engineering Technology, pp. 85–94.

Akbari, V., Naghashzadegan, M., Kouhikamali, R., Afsharpanah, F. and Yaïci, W. (2022) 'Multi-objective optimization of a small horizontal-axis wind turbine blade for generating the maximum startup torque at low wind speeds', Machines, 10(9), p. 785.

Ala, A. (2024) Numerical investigation of the effect of winglets on the flying qualities of an aircraft. [Thesis/Report].

Alyousuf, A.M. and Korkmaz, F. (2023) 'Performance investigation of wind turbines based on doubly fed induction generators with back-to-back converter', Kufa Journal of Engineering, 14(1), pp. 1–12.

Bing (2017) Fundamentals of Aircraft and Airship Design. [online] Available at: https://www.bing.com Accessed.

Calì, M., Giorgio Cacopardo, Baiamonte, G., Laudani, G. and Ambu, R. (2022) 'Efficiency optimization in medium power wind turbines: an innovative mechanical pitch control system', International Review on Modelling and Simulations (IREMOS), 15(6), p. 367.

Das, T.K. and Samad, A. (2020) 'Influence of stall fences on the performance of Wells turbine', Energy, 194, p. 116864.

Elbashbeshy, E.M.A., Asker, H.G. and Nagy, B. (2022) 'The effects of heat generation absorption on boundary layer flow of a nanofluid containing gyrotactic microorganisms over an inclined stretching cylinder', Ain Shams Engineering Journal, 13(5), p. 101690.

Gall, M., Malael, I. and Preda, D. (2022) 'Computational analysis of fence-type vertical axis wind turbines array suitable for urban architecture integration', [Conference paper], pp. 204–210.

Gopinathan, V. and Bruce Ralphin Rose, J. (2021) 'Aerodynamics with state-of-the-art bioinspired technology: Tubercles of humpback whale', Proceedings of the Institution of Mechanical Engineers, Part G: Journal of Aerospace Engineering, 235.(12)

Jha, B.K. and Samaila, G. (2023) 'Impact of exponentially decaying internal heat generation on mixed convection boundary layer slip flow from a thermally radiated vertical plate', Transactions of Indian National Academy of Engineering, 8(3), pp. 411–422.

Jung, C. and Schindler, D. (2020) 'Integration of small-scale surface properties in a new high resolution global wind speed model', Energy Conversion and Management, 210, p. 112733.

Mohamed, A., Aly, H.H. and Little, T. (2021) 'A comparative study of hourly wind speed and power forecasting using deep learning networks, Weka time series, and ARIMA algorithms for smart grid integration', [Article].

Muheisen, A.H., Yass, M.A.R. and Irthiea, I.K. (2021) 'Enhancement of horizontal wind turbine blade performance using multiple airfoils sections and fences', Journal of King Saud University - Engineering Sciences.

Nair, M.S., Arihant, V., Bhanu Priya, D. and Subramaniyam, M. (2020) 'Design and CFD analysis of horizontal axis wind turbine blade with microtab', IOP Conference Series: Materials Science and Engineering, 912, p. 022054.

Osama A. Gaheen, Aziz, M.A., Hamza, M., Kashkoush, H. and Khalifa, M.A. (2021) 'Fluid and structure analysis of wind turbine blade with winglet', Journal of Advanced Research in Fluid Mechanics and Thermal Sciences, 90(1), pp. 80–101.

RahnamayBahambary, K., Kavian-Nezhad, M.R., Komrakova, A. and Fleck, B.A. (2024) 'A numerical study of bio-inspired wingtip modifications of modern wind turbines', Energy, 292, p. 130561.

Stabilisation of Hydrodynamic Instabilities by Critical Layers in Acoustic Lining Boundary Layers (2023) AIAA Journal.

Umar, D.A., Yaw, C.T., Koh, S.P., Tiong, S.K., Alkahtani, A.A. and Yusaf, T. (2022) 'Design and optimization of a small-scale horizontal axis wind turbine blade for energy harvesting at low wind profile areas', Energies, 15(9), p. 3033.

Volpiani, P.S. (2021) 'Numerical strategy to perform direct numerical simulations of hypersonic shock/boundary-layer interaction in chemical nonequilibrium', Shock Waves, 31(4), pp. 361–378.

Xi, L. and Zhao, L. (2022) 'Optimal design of wind turbine blades by combination of multi-airfoil leaf elements', Journal of Physics: Conference Series, 2235(1), p. 012008.

Zhang, D., Liu, D., Liu, X., Xu, H., Wang, Y., Bi, R. and Qian, P. (2024) 'Unsteady effects of a winglet on the performance of horizontal-axis tidal turbine', Renewable Energy, p. 120334.